applied optics

Improving thermo-optic properties of smart windows via coupling to radiative coolers

Erjun Zhang,[1] Yang Cao,[1] Christoph Caloz,[2] and Maksim Skorobogatiy[1,*]

[1]Engineering Physics, École Polytechnique de Montréal, C. P. 6079, succ. Centre-ville, Montréal, Quebec H3C 3A7, Canada
[2]Electrical Engineering, École Polytechnique de Montréal, C. P. 6079, succ. Centre-ville, Montréal, Quebec H3C 3A7, Canada
*Corresponding author: maksim.skorobogatiy@polymtl.ca

Received 4 November 2019; revised 25 February 2020; accepted 27 February 2020; posted 28 February 2020 (Doc. ID 382050); published 31 March 2020

In this work we first solve the radiative heat transfer problem in one dimension to perform a comparative analysis of the time-averaged performance of the partially transparent radiative windows and radiative coolers. In doing so, we clearly distinguish the design goals for the partially transparent windows and radiative coolers and provide optimal choice for the material parameters to realize these goals. Thus, radiative coolers are normally non-transparent in the visible, and the main goal is to design a cooler with the temperature of its dark side as low as possible relative to that of the atmosphere. For the radiative windows, however, their surfaces are necessarily partially transparent in the visible. In the cooling mode, the main question is rather about the maximal visible light transmission through the window at which the temperature on the window somber side does not exceed that of the atmosphere. We then demonstrate that transmission of the visible light through smart windows can be significantly increased (by as much as a factor of 2) without additional heating of the windows. This is accomplished via coupling the windows to the radiative coolers using transparent cooling liquid that flows inside of the window and radiative cooler structures. We also demonstrate that efficient heat exchange between radiative coolers and smart windows can be realized using small coolant velocities (sub-1 mm/s for ∼1 m large windows) or even using a purely passive gravitationally driven coolant flows between a hot smart window and a cold radiative cooler mounted on top of the window with only a minimal temperature differential (sub-1K) between the two. We believe that our simple models complemented with an in-depth comparative analysis of the standalone and coupled smart windows and radiative coolers can be of interest to a broad scientific community pursuing research in these disciplines.

https://doi.org/10.1364/AO.382050

1. INTRODUCTION

Currently, the problem of energy overconsumption presents one of the major challenges for many societies [1]. In particular, energy spending for building cooling, heating, and lighting accounts for ∼40% of the total energy consumption in some countries [1,2]. While several methods to reduce energy use for the cooling of buildings, automobiles, food depots, and other structures are known, radiative cooling distinguishes itself by being one of the few temperature reduction methods that require no external energy sources for their operation [1,2]. The design of radiative coolers presents an intriguing multidisciplinary problem at the intersection of physics, material science, optics, and engineering.

Similar to other cooling methods, the general idea of the radiative cooling is to achieve larger energy outgoing flux than the incoming energy flux [3]. Standard passive cooling devices use large heat sinks with lower temperature than that of a cooled object to reach large outgoing energy fluxes [4]. On a planetary scale, the Earth temperature is ∼300 K, which is much larger than the temperature of the outer space ∼3 K that acts as an infinite heat sink for the planet [3]. As the outer space is a near perfect vacuum, the main heat loss mechanism for the Earth is not a conduction driven heat transfer but a radiative one. This is due to the fact that objects with temperatures above the absolute zero radiate electromagnetic energy known as thermal radiation or blackbody radiation with the spectrum depending on the object temperature and described by the Planck's law. Thus, objects with temperatures of ∼300 K mainly radiate energy in the mid-IR with a broad peak in the spectral density covering the wavelength of 8–15 μm [4]. Remarkably, in the same spectral range, the Earth's atmosphere has a transmission window (window of transparency) that allows a considerable portion of the mid-IR thermal radiation to leave unimpeded [4,5]. This represents the main mechanism by which terrestrial objects can dissipate heat into the outer space in the form of electromagnetic waves, which is the basis of radiative cooling. It is pertinent to

mention at this point that the Earth cooling via radiative heat transfer to the outer space is compensated by heating of the Earth surface via partial absorption of the radiative energy of the Sun that features the highest spectral density in the visible, while extending all the way to the near-IR 0.3–2.5 μm [6].

The study of radiative cooling has a long history. It has been well known since the ancient times that using blackened surfaces (radiators) facing a clear night sky could result in sub-ambient temperatures of the radiator, which was even used to make ice [7]. Temperature reduction of about 5°C was reported by Granqvist in 1981 [8], using a low emittance window surface and nighttime cooling. This original work was followed by several studies of radiative cooling efficiency under different environmental conditions, such as humidity [9,10], ambient temperature [11], and geographical location [12]. This original work was followed by studies of the daytime cooling, which turned to be a much harder problem. Originally, daytime radiative cooling under direct sunlight was achieved by using a radiator that would reflect most of the sunlight, while radiating efficiently in the mid-IR spectral range [13], thus allowing the heat to escape through the atmospheric transparency window. The fact that the radiative energy of the Sun and the thermal radiation of a terrestrial object occupy different and mostly non-overlapping parts of the electromagnetic spectrum makes the problem of the radiative cooler design more complicated. This is because the cooler materials have to exhibit widely different thermo-optic properties in the visible and mid-IR spectral ranges.

A large number of studies have been conducted to date on a subject of radiative cooler materials (electrochromic, photochromic windows and thermochromic windows [14–16], photonic crystals and metamaterials [13,17]), as well as structures and design optimization (reflecting versus absorbing structures [17–19]), with experimentally demonstrated temperature reduction from 5°C to 42°C [4,13,20]. Furthermore, the question of the fundamental limit in the temperature reduction for radiative coolers was investigated in great detail with a consensus that it depends strongly on the environmental conditions [10,21]. Thus, for the nighttime radiative coolers the predictions range between 15°C–42°C [21–23], while for the daytime radiative coolers the temperature reduction is expected to be only several degrees [13].

An important issue when characterizing radiating coolers is the choice of parameters to characterize the cooler performance. While the cooler itself has a working surface, its main function is to cool the air and solid objects behind it. Therefore, while the cooler surface temperature is of importance the more practical parameter is probably the air temperature or the temperature of a solid behind the cooler. Another issue is about on-average versus instantaneous performance of a cooler. While some coolers work mostly during night-time, others are capable of the day and night operation [24]. They are known as high efficiency radiative coolers or radiative windows if the cooler surface is partially transparent. Additionally, if the window can adjust its radiative properties in response to the changing environmental conditions (for example, ambient temperature, daylight illumination [25–27]), or if it is capable of both cooling and heating, such windows are frequently referred to as intelligent/smart windows [28].

Recently, there has been a strong interest in passive and active smart windows that could operate year-long, while providing heating in the cold and cooling in the hot weather [24,29]. Much research is focusing on developing materials that can simultaneously, while independently manage radiation across several widely spaced spectral ranges covering, for example, visible/near-IR light [12,30,31], or solar/mid-IR light [20]. At the same time, a concept of perfect smart window was proposed to judge the energy efficiency of the existing smart windows [32,33]. Thus, the perfect smart window has zero absorptivity for the visible light, near-infrared, and mid-infrared. At the same time, the window features a perfect transmittance in the visible, while the mid-IR light transmittance and reflectance should be either (zero, perfect) or (perfect, zero) depending on whether heating or cooling is required. In any case, to switch between the heating and cooling states the intelligent windows should allow large difference in its transmittance/reflectance properties between the two states, while always featuring low absorption of solar radiation [32]. Therefore, much attention was paid to improving smart windows through materials research and structural optimization [29,34–39].

Currently, there are three main types of smart windows in development that use electrochromic, thermochromic, photochromic materials and combinations of thereof. Electrochromic materials employ reversible redox reaction that affects material's electronic transitions, and, as a consequence, the absorption profile of the solar spectra [28]. Several metal oxides have been reported for applications in smart windows among which the tungsten oxide (WO_3) is the most popular one due to the material's fast switching time between opaque and clear sates, as well as high visible light transmission in the clear state [40,41]. Thermochromic smart windows employ materials that exhibit phase transition between the semiconducting monoclinic phase (clear state) and the metallic rutile phase (opaque state) as a function of temperature. Vanadium dioxide (VO_2)-based materials are the most popular ones to regulate transmission of the visible and near-IR light using the thermochromic effect [41]. At the same time, even in the clear state transmittance of the visible light through this material is relatively low because of the material strong absorption and reflection in the short wavelength range [40]. In addition, the VO_2 phase transition temperature ∼68°C is relatively high for the practical applications, while transition temperatures in the 20°C–30°C would be more desired. Finally, the photochromic smart window can alter its light transmission properties depending on the intensity of the incident sunlight. Photochromic materials have a large working temperature range (from 20°C to as high as 80°C), and are relatively abundant [40,42].

While much work has been done on theoretical understanding of the functioning of radiative coolers, in the related field of smart windows the performance targets and optimization strategies are still less understood. As functioning of the smart windows is dominated by the multi-year-long time scale, therefore it is interesting to analyze their averaged-over-time performance rather than an instantaneous response. It is also important to acknowledge that the function of a window implies non-zero visible light transmission; therefore, a trade-off between the window performance and its esthetic function seems unavoidable. In this respect it is interesting to investigate

the possibility of improving thermo-optical performance of smart windows via their coupling to the radiative coolers, which to our knowledge is novel.

In this paper we, therefore, consider in more detail partially transparent radiative coolers in the context of their application in smart windows. From the onset we distinguish the design goals for the radiative coolers from those of the partially transparent (in the visible) radiative windows. Thus, radiative coolers are normally non-transparent in the visible, and the main goal is to design a cooler with the temperature of its dark side as low as possible compared to that of the atmosphere. For the radiative windows, however, their surfaces are necessarily partially transparent in the visible. In the cooling mode, therefore, the main question is about the maximal visible light transmission through the window at which the temperature on the window somber side does not exceed that of the atmosphere. Alternatively, as a measure of the window performance one can use the temperature of the adjacent inner air region or even that of the room wall. Finally, by coupling the radiative window to the radiative cooler using active or passive heat exchange mechanisms (gravitationally driven coolant flow, etc.), one can increase window transmission of the visible light, while maintaining its temperature constant.

As mentioned earlier, a practical window requires that a significant amount of the visible light is transmitted through the window into the living space (see Fig. 1). This light (carrying energy flux P_{VIS}) is then absorbed on the inner walls of the building, which can be considered as gray bodies. Additionally, a window of temperature T_w itself emits mid-IR light both inside and outside of the building with energy flux $P_{\mathrm{WIN}} \sim \sigma T_w^4$. Finally, the inner walls of the building with temperature T_s will re-emit the absorbed visible light as well as the absorbed mid-IR light coming from the window back toward the window with an energy flux $P_{\mathrm{WALL}} \sim \sigma T_s^4$. Assuming that the window is made of high emissivity material (meaning essentially that all the mid-IR light incident onto the window is completely absorbed within the window thickness), then from the energy conservation at the wall interface $P_{\mathrm{VIS}} + P_{\mathrm{WIN}} = P_{\mathrm{WALL}}$. From this energy conservation relation, we conclude that one way of reducing the building wall temperature, while still having significant amount of the visible light inside the building, is by reducing the amount of the mid-IR energy flux coming from the window, or equivalently by reducing the window temperature. One passive solution to this is by thermally coupling a window to a radiative cooler. This can be realized by placing a radiative cooler panel on the outer wall of the building and allowing a coolant liquid that fills the window and radiative cooler panels to exchange between them. For example, by placing a radiative cooler panel above a window panel, the coolant liquid exchange between the two can be purely gravitationally driven as the colder liquids (in the radiative cooler) are heavier than the warmer ones (in the window panel); thus, a natural gravitationally driven convection cycle can be established in such a system. The coolant liquid should be relatively transparent in the visible spectral range in order to prevent additional window heating due to light absorption in the coolant, while the window panel can be integrated directly with the radiative cooler, as shown in Fig. 1. Later in the paper we consider in more detail conditions necessary for an efficient gravitationally driven

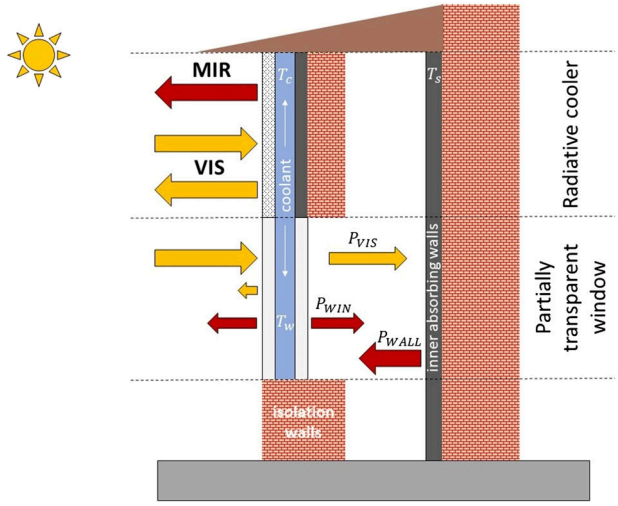

Fig. 1. Schematic of the window/radiative cooler tandem.

coolant exchange between the window and radiative cooler panels. There, we conclude that efficient passive window cooling is indeed possible when using radiative cooler and window panels of comparable size $L \sim 1$ m and assuming that temperature differential between the two panels is higher than a fraction of a degree $T_w - T_c \gtrsim 1$ K, which is easy to realize in practice even under the daylight conditions using relatively simple radiative cooler designs. We believe that proposed solution is particularly suitable for installation in the high-rise buildings as in such a case radiative cooler panels have, and unobstructed view of the sky and their efficiency are expected to be higher than in the case of lower buildings.

In order to model precisely the smart window performance, one has to have a realistic model of the atmospheric optical properties [43], and then solve a full radiative heat transfer problem [44] that includes atmosphere, window, and enclosure where the window is installed. While certainly possible, such an overwhelming approach will most probably obscure the relatively simple physics behind the problem. Therefore, in this work we strip the radiative heat transfer problem to a bare minimum and confine ourselves to one dimension, while still retaining all the key elements of a problem. Particularly, we consider the atmosphere, the window, the cooler, and the back wall that are all in the thermal equilibrium and that all exchange the energy via radiative heat transfer, convection, or coolant flow. Moreover, we use a simplified two-state model for the optical properties of an atmosphere and a window material that assumes two distinct sets of the optical reflection/absorption/transmission parameters in the visible/near-IR and mid-IR spectral ranges. Furthermore, we assume constant temperature across the radiative window/cooler, which is justified for materials with relatively high thermal conductivity. Finally, heat exchange between the window and a radiative cooler is modeled via fixed volumetric rate coolant flow between the internal elements of their structure. We believe that our work captures all the important aspects of the radiative heat transfer in smart windows and allows us to make valuable qualitative predictions on the choice of the windows optimal design parameters without resorting to solution of the overcomplicated full radiative transfer problem.

2. SINGLE-LAYER MODEL OF THE ATMOSPHERE

We start with a single-layer model of the atmosphere [45] (see Fig. 2). This model allows us to relate together the Earth and the atmosphere average temperatures (T_g and T_a), the atmosphere average emissivity $\varepsilon_a(\nu)$, the planet albedo al (reflectivity of the atmosphere and Earth surface), and the total incoming radiative flux from the Sun $P(\nu)$. This model is a necessary point of departure that allows definition of a self-consistent reference (average atmospheric properties versus average Sun radiative flux) for the following models of smart windows. The model assumes equilibrium temperature distribution, and, hence, net zero radiative heat flux through any interface parallel to the Earth. A key element of the model is a recognition that in equilibrium, the material absorption coefficient equals to the material emission coefficient. Namely, $\varepsilon_a(\nu)$ - the emissivity of the atmosphere at frequency ν equals to its absorption $\alpha_a(\nu)$ as $\varepsilon_a(\nu) = \alpha_a(\nu) = 1\text{-}r_a(\nu)\text{-}t_a(\nu)$. Here, $r_a(\nu)$ is the atmospheric reflection coefficient (mostly due to Rayleigh scattering), $t_a(\nu)$ is the atmospheric transmission coefficient $t_a(\nu) \approx (1\text{-}r_a(\nu))\exp(\text{-}\alpha_a(\nu)L_a)$, where L_a is the atmosphere thickness, and $\alpha_a(\nu)$ is the atmosphere absorption coefficient. Finally, we assume that emissivity of the Earth at any frequency is 1 (blackbody) and define the emission spectrum (by power) of a blackbody at temperature T as $E(\nu, T)$.

A detailed study of this model (see, for example, [46]) shows that the atmospheric temperature T_a is related to the ground temperature T_g and the average radiative flux from the Sun incident onto the planet $\bar{P}$ as

$$\sigma T_a^4 = \frac{(1-al)}{(2-\varepsilon_a)}\bar{P},\ T_g = 2^{1/4}\cdot T_a, \tag{1}$$

where we assume that the power of the incoming light from the Sun is mostly concentrated in the UV/visible/near-IR spectral range (wavelengths of 250 nm–3 μm), while the power of the irradiated light by the atmosphere and Earth are mostly in the mid-IR spectral range (wavelengths 3 μm–30 μm), with little overlap between the two. Therefore, instead of using frequency-variable transmission and reflection properties of the atmosphere, we rather assume a step-like spectral behavior of its optical properties with albedo al defining a spectrally averaged (over visible) atmospheric reflection, while ε_a defines a spectrally average (over mid-IR) atmospheric absorption. In order to reproduce with this model the average Earth temperature $T_g = 288.2$ K, while using for the planet albedo $al = 0.3$, and the average radiative flux from the Sun incident onto the planet $\bar{P} = 342\ \mathrm{W}\cdot\mathrm{m}^{-2}$ (which factors in the fact that half of the planet is illuminated at any given time, as well as non-normal incidence of the solar light onto different regions of the planet surface) one requires to choose for the atmosphere emissivity $\varepsilon_a = 0.78$. This also results in a somewhat low atmospheric temperature $T_a = 242.11$ K (−30°C), which is a well-known deficiency of a single-layer atmospheric model. Note that the quoted value for the average incoming solar radiation takes into account the angle at which the rays strike and that at any one moment half the planet does not receive any solar radiation. It therefore measures only one fourth of the solar constant, which is an averaged over the year energy flux incident on the Earth as measured from space.

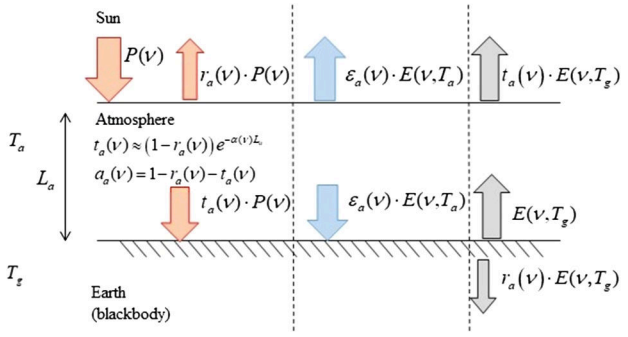

Fig. 2. Single-layer model of the atmosphere with the corresponding energy fluxes at the two interfaces.

3. SINGLE-LAYER, PARTIALLY TRANSPARENT RADIATIVE WINDOW

We now consider a single-layer optically symmetric window placed in the path of a sunlight [see Fig. 3(a)]. We note that the 3D nature of the world and details of the local environment will have an impact on the performance of the window and radiative cooler. As in this paper we rather aim at simplified physical description of the novel window/radiative cooler tandem rather than a detailed modeling of the realistic performance of such a system, we resorted to analysis of the worst-case scenario for the cooler performance. In particular, we assume that the house interior is covered with a dark paint that absorbs all the visible light, while the window is oriented perpendicular to the incident sunlight, so that the total of the average solar flux is incident onto the window. At the same time, we suppose that the window has a full access to the sky, which is most realistically the case for a high-rise building rather than a small house where reflections from the ground and surroundings could reduce the radiative cooler performance.

Furthermore, the window is assumed to be optically thick (no interference effects). We also assume that the temperature across the window is constant and equal to T_w, and, therefore, the thermal radiation from the window is the same in both directions. Validity of this approximation is studied, for example, in Ref. [46], Supplementary Material A, where a full radiative heat transfer model is solved for a standalone slab and it is demonstrated that temperature inside can be considered constant if the slab is made of material with high enough thermal conductivity. Behind the window we place a perfect absorber that we refer to as a wall, and the temperature of the wall surface behind the window, which is considered to be a blackbody, is represented by T_s. The wall is assumed to be thermally and radiationally separated from the ground. We, furthermore, assume that there is vacuum between the window and the wall, so we neglect the convection and conduction heat transfer in this region. Finally, the Earth atmosphere is characterized by the average temperature and emissivity defined earlier.

Spectral dependence of the window material parameters ($r_w(\nu)$, $t_w(\nu)$, $\alpha_w(\nu)$) are assumed to be step-like, with two distinct sets of frequency-independent parameters defining window properties in the mid-IR and visible ranges, as shown in Fig. 3(b). The spectrum of the incoming radiation from the Sun

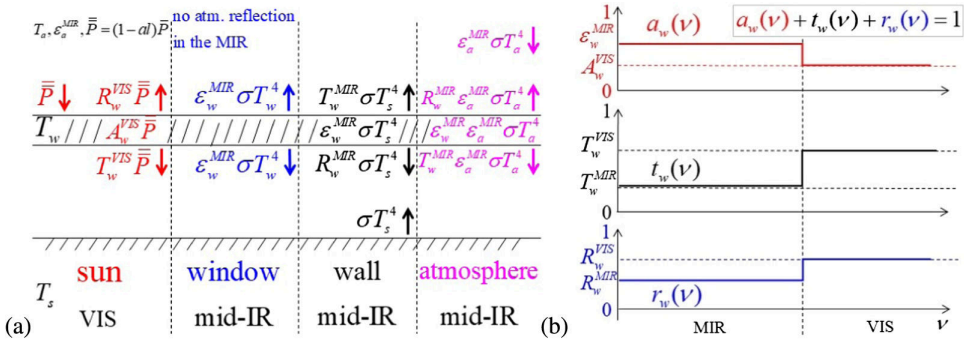

Fig. 3. (a) Model of the optically symmetric single-layer window (no convection/conduction between the wall and the window). (b) Step-like model for the frequency-dependent optical properties of the window (absorption, transmission, and reflection).

at the ground level by power is given by $P_g(\nu) = t_a(\nu) \cdot P(\nu)$, and the average power of the Sun at the planet (window) surface is given by $\bar{\bar{P}} = (1-al)\,\bar{P}$. Using the energy conservation principle at different interfaces and following derivations of Ref. [46], we can relate the average atmospheric temperature to the average thermal properties of the atmosphere and window as

$$\frac{T_w^4}{T_a^4} = \varepsilon_a + (2-\varepsilon_a)\frac{T_w^{\mathrm{VIS}} + A_w^{\mathrm{VIS}} \cdot \left(1 + \frac{T_w^{\mathrm{MIR}}}{\varepsilon_w^{\mathrm{MIR}}}\right)}{2\,T_w^{\mathrm{MIR}} + \varepsilon_w^{\mathrm{MIR}}},$$

$$\frac{T_s^4}{T_a^4} = \varepsilon_a + (2-\varepsilon_a)\frac{2\,T_w^{\mathrm{VIS}} + A_w^{\mathrm{VIS}}}{2\,T_w^{\mathrm{MIR}} + \varepsilon_w^{\mathrm{MIR}}}. \tag{2}$$

The radiative heat transfer model for a single-layer partially transparent window can be readily extended to account for the convection heat transfer between the window and the air that surrounds it. The resultant model is virtually identical to the one presented in this section and includes only two new parameters, which are the room temperature (in the space between the window and the wall) and the heat transfer coefficient h. For completeness, we detail this model extension and its analysis in Ref. [46], Supplementary Material B. The key conclusion derived from analysis of this model is that convection heat transfer always reduces efficiency of the radiative coolers and windows more so for stronger convection rates. Convection contribution becomes important for large enough values of the heat transfer coefficient $h/(8\sigma T_a^3) > (2\,T_w^{\mathrm{MIR}} + \varepsilon_w^{\mathrm{MIR}})$, which is equivalent to $h > 6.46\,[\mathrm{W/K}] \cdot (2\,T_w^{\mathrm{MIR}} + \varepsilon_w^{\mathrm{MIR}})$ when operating in the vicinity of standard ambient temperatures. The value of the heat transfer coefficient depends strongly on the temperature differential, as well as the window size and orientation and is generally in the 1–10[W/K] range (see Ref. [46], Supplementary Material C for more details).

A. Analysis of the Thermal Properties of a Single-Layer Radiative Window

Here we present the performance analysis of various radiative windows as predicted by the model presented in the previous section. In particular, we study the trade-off between transmission of the visible light through the radiative window and its temperature, as well as the wall temperature behind the window.

First, we inquire about the smallest wall temperature T_s possible. From Eq. (2) we find

$$\begin{aligned}
&\min(T_s) = \varepsilon_a^{1/4} \cdot T_a \approx 0.94 \cdot T_a \\
&\text{when } \frac{2T_w^{\mathrm{VIS}} + A_w^{\mathrm{VIS}}}{2T_w^{\mathrm{MIR}} + \varepsilon_w^{\mathrm{MIR}}} = 0 \\
&\Rightarrow T_w^{\mathrm{VIS}} \to 0;\ A_w^{\mathrm{VIS}} \to 0 \Rightarrow R_w^{\mathrm{VIS}} \to 1 \\
&\text{we must also require } 2\,T_w^{\mathrm{MIR}} + \varepsilon_w^{\mathrm{MIR}} = \\
&\quad = 1 + T_w^{\mathrm{MIR}} - R_w^{\mathrm{MIR}} \neq 0 \Rightarrow R_w^{\mathrm{MIR}} \neq 1.
\end{aligned} \tag{3}$$

This is the case of an almost completely reflective window in the visible, which at the same time has a non-perfect reflectivity in the mid-IR.

Second, we study the smallest window temperature T_w possible. From Eq. (2) we find that

$$\begin{aligned}
&\min(T_w) = \varepsilon_a^{1/4} \cdot T_a \approx 0.94 \cdot T_a \\
&\text{when } \frac{T_w^{\mathrm{VIS}} + A_w^{\mathrm{VIS}} \cdot \left(1 + \frac{T_w^{\mathrm{MIR}}}{\varepsilon_w^{\mathrm{MIR}}}\right)}{2\,T_w^{\mathrm{MIR}} + \varepsilon_w^{\mathrm{MIR}}} = 0 \Rightarrow T_w^{\mathrm{VIS}} \to 0;\ A_w^{\mathrm{VIS}} \to 0; \\
&\quad \frac{A_w^{\mathrm{VIS}}}{\varepsilon_w^{\mathrm{MIR}}} \to 0 \Rightarrow R_w^{\mathrm{VIS}} \to 1; \quad A_w^{\mathrm{VIS}} \ll \varepsilon_w^{\mathrm{MIR}} \\
&\text{we must also require } 2\,T_w^{\mathrm{MIR}} + \varepsilon_w^{\mathrm{MIR}} = \\
&\quad = 1 + T_w^{\mathrm{MIR}} - R_w^{\mathrm{MIR}} \neq 0 \Rightarrow R_w^{\mathrm{MIR}} \neq 1.
\end{aligned} \tag{4}$$

This is the case of an almost completely reflective window in the visible, which at the same time has a non-perfect reflectivity in the mid-IR. Additionally, we have to require that the window absorption in the visible is much smaller than the window absorption in the mid-IR.

Next, we study the maximal transmission of the visible light through the window T_w^{VIS} so that the wall temperature does not exceed the atmospheric temperature $T_s < T_a$. From Eq. (2), we find that

$$\begin{aligned}
&\frac{T_s^4}{T_a^4} = \varepsilon_a + (2-\varepsilon_a)\frac{2T_w^{\mathrm{VIS}} + A_w^{\mathrm{VIS}}}{2T_w^{\mathrm{MIR}} + \varepsilon_w^{\mathrm{MIR}}} < 1, \\
&T_w^{\mathrm{VIS}} < \tfrac{1}{2}\tfrac{1-\varepsilon_a}{2-\varepsilon_a}\left(1 + T_w^{\mathrm{MIR}} - R_w^{\mathrm{MIR}}\right) - \frac{A_w^{\mathrm{VIS}}}{2}, \\
&\max\left(T_w^{\mathrm{VIS}}\right) = \gamma \quad \text{when } T_w^{\mathrm{MIR}} = 1 \left(\varepsilon_w^{\mathrm{MIR}} = R_w^{\mathrm{MIR}} = 0\right); \\
&\quad A_w^{\mathrm{VIS}} = 0, \\
&\text{where} \gamma = \tfrac{1-\varepsilon_a}{2-\varepsilon_a} = 0.18.
\end{aligned} \tag{5}$$

In order to achieve maximal transmission of the visible light, while still having the wall temperature below that of the atmosphere, we have to demand that window absorption in the visible is zero $A_w^{\mathrm{VIS}} \to 0$, while window transmission in the mid-IR is almost perfect $T_w^{\mathrm{MIR}} \to 1$.

Finally, we study the maximal transmission of the visible light through the window T_w^{VIS}, so that the window temperature does not exceed the atmospheric temperature $T_w < T_a$. From Eq. (2) it follows that

$$\begin{aligned}
&\frac{T_w^4}{T_a^4} = \varepsilon_a + (2-\varepsilon_a)\frac{T_w^{\mathrm{VIS}} + A_w^{\mathrm{VIS}} \cdot \left(1 + \frac{T_w^{\mathrm{MIR}}}{\varepsilon_w^{\mathrm{MIR}}}\right)}{2\,T_w^{\mathrm{MIR}} + \varepsilon_w^{\mathrm{MIR}}} < 1,\\
&T_w^{\mathrm{VIS}} < \frac{1-\varepsilon_a}{2-\varepsilon_a}\left(1 + T_w^{\mathrm{MIR}} - R_w^{\mathrm{MIR}}\right) - A_w^{\mathrm{VIS}} \cdot \left(1 + \frac{T_w^{\mathrm{MIR}}}{\varepsilon_w^{\mathrm{MIR}}}\right),\\
&\max\left(T_w^{\mathrm{VIS}}\right) = 2\gamma = 0.36 \text{ when } T_w^{\mathrm{MIR}} \to 1\left(\varepsilon_w^{\mathrm{MIR}},\ R_w^{\mathrm{MIR}} \to 0\right);\\
&\quad A_w^{\mathrm{VIS}} \ll \varepsilon_w^{\mathrm{MIR}} \to 0.
\end{aligned} \tag{6}$$

In order to achieve maximal transmission of the visible light, while still having the window temperature below that of the atmosphere, we have to demand that window transmission in the mid-IR is almost perfect $T_w^{\mathrm{MIR}} \to 1$, while window absorption in the visible is much smaller than that in the mid-IR, and at the same time approaching zero $A_w^{\mathrm{VIS}} \to 0$.

4. PARTIALLY TRANSPARENT SMART WINDOW THERMALLY COUPLED TO A RADIATIVE COOLER

An idea that we explore in this section is to exploit the cooling properties of passive radiative coolers in order to enhance transmission of the visible light through the smart windows, without increasing the window temperature or the temperature of the wall behind it. This idea can be of practical significance as there were recent reports of successful cooling of water (coolant) flowing through the internal structure of a radiative cooler [47]. In particular, we envision a transparent (in the visible) coolant that passively or actively flows through the window and the radiative cooler inner structures (see Fig. 4). The coolant carries the heat from the partially transparent window which is then dissipated into the atmosphere by the radiative cooler. The goal of this section is to quantify the potential improvements in the intensity of transmitted visible light through the window offered by such a hybrid structure.

As established in the previous sections, there is a trade-off between the transmitted intensity of the visible light and the temperature of the window and the back wall. For example, we have established that the maximal transmission of the visible light through the window T_w^{VIS}, so that the window temperature does not exceed the atmospheric temperature $T_w < T_a$, equals to $\max(T_w^{\mathrm{VIS}}) = 2\gamma$, where $\gamma = (1-\varepsilon_a)/(2-\varepsilon_a) = 0.18$ and we have to demand that the window absorption in the visible is zero $A_w^{\mathrm{VIS}} \to 0$, while window transmission in the mid-IR is almost perfect $T_w^{\mathrm{MIR}} \to 1$. Additionally, we have established that in the case of radiative coolers, the cooler temperature can be made significantly smaller than that of the atmosphere $\min(T_w) = \varepsilon_a^{1/4}\, T_a \approx 0.94 \cdot T_a$ by requiring that the cooler surface is almost completely reflective in the visible, and that the radiative cooler absorption in the visible is much smaller than the window absorption in the mid-IR. In what follows we explore a scenario where a smart window and a radiative cooler are thermally coupled. In this case, a radiative cooler is used to reduce the temperature of a smart window, which, in turn, allows to increase the intensity of transmitted visible light through the window, without increasing the window temperature beyond that of the atmosphere.

In particular, we consider two channels, one inside of a smart window and another one inside a radiative cooler, that contain a transparent (in the visible coolant) fluid such as water or oil characterized by the volume heat capacity C_v. We suppose that the liquid flows in a closed loop between a smart window and a radiative cooler with a flow speed v_f, and that both channels have the same cross-section area $A_{\mathrm{channel}} \sim L \cdot d$, while both the cooler and the window have the same radiative areas $A_{\mathrm{rad.area}} \sim L^2$, where L is a characteristic window/cooler size, and d is the coolant channel size. Then, the heat transfer rate (per unit area) from the window Q_w and the cooler Q_c can be defined as

$$Q_w = \zeta \cdot T_w;\ Q_c = \zeta \cdot T_c, \tag{7}$$

where the heat transfer rate per unit temperature is defined as $\zeta = C_v \cdot A_{\mathrm{channel}} \cdot v_f / A_{\mathrm{rad.area}}$ [W/(m^{2}K)]. Then, using energy conservation of the radiative and thermal fluxes we can get the modified system of equations that describe the coupled window/radiative cooler system similar to that presented in the previous sections. Thus, using subscripts c to indicate cooler variables, while using subscript w to indicate window variables (also see Fig. 4), we write

$$\begin{cases}
A_w^{\mathrm{VIS}} \cdot \bar{\bar{P}} + \varepsilon_w^{\mathrm{MIR}} \cdot \sigma\, T_{sw}^4 + \varepsilon_w^{\mathrm{MIR}} \cdot \varepsilon_a \sigma\, T_a^4 + (T_c - T_w) \cdot \zeta = 2\varepsilon_w^{\mathrm{MIR}} \cdot \sigma\, T_w^4\\
T_w^{\mathrm{VIS}} \cdot \bar{\bar{P}} + T_w^{\mathrm{MIR}} \cdot \varepsilon_a \sigma\, T_a^4 + \varepsilon_w^{\mathrm{MIR}} \cdot \sigma\, T_w^4 = \left(1 - R_w^{\mathrm{MIR}}\right) \cdot \sigma\, T_{sw}^4\\
A_c^{\mathrm{VIS}} \cdot \bar{\bar{P}} + \varepsilon_c^{\mathrm{MIR}} \cdot \sigma\, T_{sc}^4 + \varepsilon_c^{\mathrm{MIR}} \cdot \varepsilon_a \sigma\, T_a^4 + (T_w - T_c) \cdot \zeta = 2\varepsilon_c^{\mathrm{MIR}} \cdot \sigma\, T_c^4\\
T_c^{\mathrm{VIS}} \cdot \bar{\bar{P}} + T_c^{\mathrm{MIR}} \cdot \varepsilon_a \sigma\, T_a^4 + \varepsilon_c^{\mathrm{MIR}} \cdot \sigma\, T_c^4 = \left(1 - R_c^{\mathrm{MIR}}\right) \cdot \sigma\, T_{sc}^4
\end{cases} \tag{8}$$

While the analytical solution of Eq. (8) is possible after linearization of the fourth-order temperature terms, due to large number of materials coefficients, the resultant expressions are complicated. To demonstrate how coupling of a radiative cooler to a window can result in the window enhanced transmission properties, we first consider a particular case of strongly absorbing in the mid-IR cooler and window materials $\varepsilon_w^{\mathrm{MIR}} = \varepsilon_c^{\mathrm{MIR}} = 1$. Moreover, for the radiative cooler we suppose that all the visible radiation is reflected without absorption $T_c^{\mathrm{VIS}} = A_c^{\mathrm{VIS}} = 0$. Finally, we suppose that window material

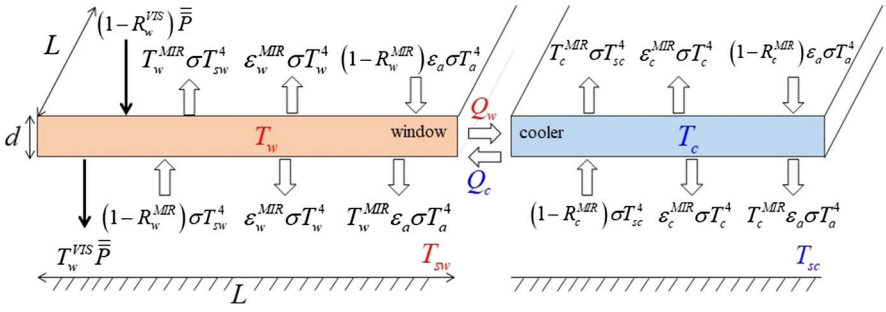

Fig. 4. Thermally coupled radiative cooler and partially transparent window via exchange of a cooling fluid. Thus, cooled windows can offer higher transmission intensities of the visible light compared to a standalone window.

does not absorb visible light $A_w^{\mathrm{VIS}}=0$. In this case one can demonstrate that $T_{sc}=T_c$, while Eq. (5) can be simplified as follows:

$$\begin{cases} \frac{T_w^4}{T_a^4}=T_w^{\mathrm{VIS}}\cdot\frac{\bar{\bar{P}}}{\sigma T_a^4}+\varepsilon_a+\left(\frac{T_c}{T_a}-\frac{T_w}{T_a}\right)\cdot\frac{\zeta}{\sigma T_a^3} \\ \frac{T_{sw}^4}{T_a^4}=2\cdot T_w^{\mathrm{VIS}}\cdot\frac{\bar{\bar{P}}}{\sigma T_a^4}+\varepsilon_a+\left(\frac{T_c}{T_a}-\frac{T_w}{T_a}\right)\cdot\frac{\zeta}{\sigma T_a^3} \\ \frac{T_c^4}{T_a^4}=\varepsilon_a+\left(\frac{T_w}{T_a}-\frac{T_c}{T_a}\right)\cdot\frac{\zeta}{\sigma T_a^3} \end{cases} \tag{9}$$

Linearizing Eq. (9) around T_a by using $T^4=(T_a+\delta T)^4\approx T_a^4+4T_a^3\cdot\delta T$ and remembering expression for $\bar{\bar{P}}=(2-\varepsilon_a)\cdot\sigma T$ from a single-layer model of the atmosphere, Eq. (9) can be rewritten in the following form:

$$\begin{cases} \frac{\delta T_w}{T_a}=-\frac{1-\varepsilon_a}{4}+T_w^{\mathrm{VIS}}\cdot\frac{2-\varepsilon_a}{8}\left(1+\left(1+\frac{\zeta}{2\sigma T_a^3}\right)^{-1}\right) \\ \frac{\delta T_{sw}}{T_a}=-\frac{1-\varepsilon_a}{4}+T_w^{\mathrm{VIS}}\cdot\frac{2-\varepsilon_a}{8}\left(3+\left(1+\frac{\zeta}{2\sigma T_a^3}\right)^{-1}\right) \\ \frac{\delta T_c}{T_a}=-\frac{1-\varepsilon_a}{4}+T_w^{\mathrm{VIS}}\cdot\frac{2-\varepsilon_a}{8}\left(1-\left(1+\frac{\zeta}{2\sigma T_a^3}\right)^{-1}\right) \end{cases} \tag{10}$$

Thus, in the case of no heat exchange between the radiative cooler and a window $\zeta=0$ we retrieve the results of Section 2, while in the case of efficient heat exchange between the radiative cooler and a window $\zeta/2\sigma T_a^3\gg 1$ we find that both the window and the wall (behind the window) temperatures have decreased, while the temperature of the cooler surface has increased:

$$\underbrace{\begin{aligned}\frac{\delta T_w}{T_a}&=-\frac{1-\varepsilon_a}{4}+T_w^{\mathrm{VIS}}\cdot\frac{2-\varepsilon_a}{8}\cdot 2\\ \frac{\delta T_{sw}}{T_a}&=-\frac{1-\varepsilon_a}{4}+T_w^{\mathrm{VIS}}\cdot\frac{2-\varepsilon_a}{8}\cdot 4\\ \frac{\delta T_c}{T_a}&=-\frac{1-\varepsilon_a}{4}\end{aligned}}_{\text{no heat exchange between window and cooler } \zeta=0} \rightarrow \underbrace{\begin{aligned}\frac{\delta T_w}{T_a}&=-\frac{1-\varepsilon_a}{4}+T_w^{\mathrm{VIS}}\cdot\frac{2-\varepsilon_a}{8}\cdot 1\\ \frac{\delta T_{sw}}{T_a}&=-\frac{1-\varepsilon_a}{4}+T_w^{\mathrm{VIS}}\cdot\frac{2-\varepsilon_a}{8}\cdot 3\\ \frac{\delta T_c}{T_a}&=\frac{\delta T_w}{T_a}\end{aligned}}_{\text{strong heat exchange between window and cooler } \zeta\gg 2\sigma T_a^3} \tag{11}$$

From Eq. (11) it also follows that maximal visible transmission through the window can be increased in the case of a coupled radiative cooler/window system, while still maintaining the window and the wall (behind the window) temperatures below that of the atmosphere. For example, in the case of a standalone window, from Eq. (11) it follows that both the wall and the window temperatures are smaller than the atmosphere δT_w, $\delta T_{sw}<0$ as long as $T_w^{\mathrm{VIS}}<\gamma/2\approx 0.09$. At the same time, for the thermally coupled window and radiative cooler, it follows from Eq. (11) that both the wall and the window temperatures are smaller than that of the atmosphere as long as $T_w^{\mathrm{VIS}}<2\gamma/3\approx 0.12$, which is a significant improvement over the uncoupled case.

We remind the reader that the goal of this work is to show that when coupling the window to a radiative cooler, transmission of the visible light through the window can be increased, while maintaining the temperature inside the building unchanged. Another way of summarizing finding of this section is to note that significant improvement in the amount of transmitted light without increase in the internal wall temperature can be potentially achieved under the condition of efficient heat exchange $\zeta/2\sigma T_a^3\gg 1$ between the window and a cooler. In particular, when using strongly emissive materials both in the cooler and window panels $\varepsilon_w^{\mathrm{MIP}}=\varepsilon_c^{\mathrm{MIP}}=1$ (such as soda-lime glass, for example), while assuming an ideal radiative cooler that reflects all the visible light $R_c^{\mathrm{VIS}}=0$, as well as an ideal window that does not absorb any visible light $A_w^{\mathrm{VIS}}=0$, then as follows from Eq. (11), in the coupled system one can increase the intensity of the transmitted visible light by 4/3 (33%) compared to that of a standalone window without increasing the temperature of the internal walls or a window itself.

A. Visible Transmission Enhancement of a Smart Window Coupled to a Radiative Cooler as a Function of Heat Exchange Efficiency between Two General Cases

Finally, in the general case of non-linear Eq. (8), the analytical solution can still be found in the limit of strong heat exchange $\zeta/(4\sigma T_a^3)\gg(\varepsilon_w^{\mathrm{MIR}}\varepsilon_c^{\mathrm{MIR}})^{0.5}$ [this condition can be derived in a general case by linearizing non-linear terms in Eq. (8)]. Indeed, in that case the temperature of the window will be equal to the temperature of the radiative cooler and to that of the cooler fluid $T_w\approx T_c=T_f$, and the system Eq. (8) can be simplified by adding the first and the third equations to give

$$\begin{cases} \left(A_w^{\mathrm{VIS}}+A_c^{\mathrm{VIS}}\right)\cdot\bar{\bar{P}}+\left(\varepsilon_w^{\mathrm{MIR}}+\varepsilon_c^{\mathrm{MIR}}\right)\cdot\varepsilon_a\sigma T_a^4+\varepsilon_w^{\mathrm{MIR}}\cdot\sigma T_{sw}^4+\varepsilon_c^{\mathrm{MIR}}\cdot\sigma T_{sc}^4=2\left(\varepsilon_w^{\mathrm{MIR}}+\varepsilon_c^{\mathrm{MIR}}\right)\cdot\sigma T_f^4 \\ T_w^{\mathrm{VIS}}\cdot\bar{\bar{P}}+T_w^{\mathrm{MIR}}\cdot\varepsilon_a\sigma T_a^4+\varepsilon_w^{\mathrm{MIR}}\cdot\sigma T_f^4=(1-R_w^{\mathrm{MIR}})\cdot\sigma T_{sw}^4 \\ T_c^{VIS}\cdot\bar{\bar{P}}+T_c^{\mathrm{MIR}}\cdot\varepsilon_a\sigma T_a^4+\varepsilon_c^{\mathrm{MIR}}\cdot\sigma T_f^4=(1-R_c^{\mathrm{MIR}})\cdot\sigma T_{sc}^4 \end{cases} \tag{12}$$

Remembering the expression for $\bar{\bar{P}}=(2-\varepsilon_a)\sigma T_a^4$ from a single-layer model of the atmosphere, the system of Eq. (12) can then be solved analytically to give

$$\begin{aligned} &\text{limit of strong heat exchange } \zeta/4\sigma T_a^3\gg 1: \\ &\left.\frac{T_w^4}{T_a^4}\right|_{\zeta\to\infty}=\left.\frac{T_c^4}{T_a^4}\right|_{\zeta\to\infty}=\varepsilon_a+(2-\varepsilon_a)\cdot\frac{T_w^{\mathrm{VIS}}+A_w^{\mathrm{VIS}}\cdot\left(1+\frac{T_w^{\mathrm{MIR}}}{\varepsilon_w^{\mathrm{MIR}}}\right)+T_c^{\mathrm{VIS}}+A_c^{\mathrm{VIS}}\cdot\left(1+\frac{T_c^{\mathrm{MIR}}}{\varepsilon_c^{\mathrm{MIR}}}\right)}{2T_w^{\mathrm{MIR}}+\varepsilon_w^{\mathrm{MIR}}+2T_c^{\mathrm{MIR}}+\varepsilon_c^{\mathrm{MIR}}}; \\ &\text{no heat exchange } \zeta=0: \\ &\left.\frac{T_w^4}{T_a^4}\right|_{\zeta=0}=\varepsilon_a+(2-\varepsilon_a)\,\frac{T_w^{\mathrm{VIS}}+A_w^{\mathrm{VIS}}\cdot\left(1+\frac{T_w^{\mathrm{MIR}}}{\varepsilon_w^{\mathrm{MIR}}}\right)}{2T_w^{\mathrm{MIR}}+\varepsilon_w^{\mathrm{MIR}}};\ \left.\frac{T_c^4}{T_a^4}\right|_{\zeta=0}=\varepsilon_a+(2-\varepsilon_a)\,\frac{T_c^{\mathrm{VIS}}+A_c^{\mathrm{VIS}}\cdot\left(1+\frac{T_c^{\mathrm{MIR}}}{\varepsilon_c^{\mathrm{MIR}}}\right)}{2T_c^{\mathrm{MIR}}+\varepsilon_c^{\mathrm{MIR}}} \end{aligned} \tag{13}$$

From Eq. (13) it follows that the temperature of a smart window in the limit of strong heat exchange with a radiative cooler will always be smaller than that of a standalone window $T_w|_{\zeta\to\infty}<T_w|_{\zeta=0}$ as long as the temperature of a standalone radiative cooler is smaller than that of a standalone window $T_c|_{\zeta=0}<T_w|_{\zeta=0}$.

B. Potential Realization of the Strong Heat Exchange Regime between Smart Windows and Radiative Coolers

Here, we consider several practical examples of the forced and the gravitationally driven heat exchanges between a smart window and a radiative cooler of characteristic size $L\sim 1$ m. We suppose that the heat transfer between the two is realized via exchange of a coolant that flows across the edge of the window and into the cooler (see Fig. 4). Assuming that the coolant fluid of volumetric heat capacity $C_v\sim 4\cdot 10^6\,\mathrm{J/(m^3K)}$ (water) flows through a channel of size $d\sim 3$ mm (and width $\sim L$), then the coolant flow speed necessary to realize the regime of strong heat exchange is given by

$$\begin{aligned} &\zeta=C_v\cdot\frac{A_{\mathrm{channel}}}{A_{\mathrm{rad.area}}}\cdot v_f=C_v\cdot\frac{d}{L}\cdot v_f\gg 4\sigma T_a^3 \\ &\Rightarrow v_f\gg\frac{4\sigma T_a^3}{C_v}\cdot\frac{L}{d}\sim 0.5\ \mathrm{mm/s}. \end{aligned} \tag{14}$$

We note that thus found coolant speed is quite modest and can be easily realized via passive gravitationally driven liquid flow. Indeed, by mounting a radiative cooler of temperature T_c on top of a smart window of temperature T_w, due to coolant density dependence on temperature, this arrangement will produce a pressure differential across the window/cooler assembly:

$$\Delta P=(\rho(T_c)-\rho(T_w))gL\sim\rho(T_a)gL\cdot\alpha_f\cdot(T_c-T_w), \tag{15}$$

where the cooler fluid thermal expansion coefficient is $\alpha_f\sim 2\cdot 10^{-4}$ (water), coolant density at the ambient temperature is $\rho(T_a)\sim 10^3\,\mathrm{kg/m^3}$ (water), and a freefall acceleration is $g\approx 9.8\,\mathrm{m/s^2}$. This pressure differential then drives an upward flow of the hot coolant from a smart window and a downward flow of the cold coolant from a radiative cooler. For the coolant flow confined to a narrow channel of size d, and assuming that the channel width is comparable to the channel length $\sim L$ one can then define the channel hydraulic resistance as $R_c=12\,\mu/\mathrm{d}^3$, where the coolant viscosity is $\mu\sim 10^{-3}\,[\mathrm{Pa\cdot s}]$ (water). The hydrolic resistance can then be used to relate the pressure differential across the channel to the volume flow rate through the channel $\partial V/\partial t\,[\mathrm{m^3/s}]$, or equivalently to the gravitationally driven heat transfer rate (per unit area, per unit temperature) through the channel as follows:

$$\begin{aligned} &\frac{\partial V}{\partial t}=\frac{\Delta P}{R_c}\Rightarrow\zeta_{\mathrm{grav}}=\frac{C_v}{A_{\mathrm{rad.surface}}}\frac{\partial V}{\partial t}=\frac{C_v}{A_{\mathrm{rad.surface}}}\frac{\Delta P}{R_c} \\ &\zeta_{\mathrm{grav}}\sim\frac{\rho(T_a)C_v g\alpha_f}{12\mu}\cdot\frac{d^3}{L}\cdot(T_c-T_w). \end{aligned} \tag{16}$$

Finally, in order to realize the strong heat exchange regime between a smart window and a radiative cooler using only gravitationally driven flow we must demand that

$$\zeta_{\mathrm{grav}}\gg 4\sigma T_a^3\Rightarrow(T_c-T_w)\gg\frac{48\sigma T_a^3\mu}{\rho(T_a)C_v g\alpha_f}\frac{L}{d^3}\underset{\text{water}}{\sim}0.35\ \mathrm{K}. \tag{17}$$

As follows from Eq. (17), efficient heat exchange between a smart window and a radiative cooler is possible to realize by simply mounting one on top of the other and using a completely passive gravitationally driven flow, as long as the temperature differential between the cooler and a window is larger than a fraction of one degree. Considering that standard radiative coolers can achieve temperatures that are tens of degrees below that of the ambient, then even under the daylight illumination conditions, we believe that the proposed gravitationally driven heat exchange mechanism is viable.

5. DISCUSSION

Here we discuss advantages and limitations of the window/radiative cooler tandem solution and compare them to

those of the technologically simpler standalone radiative coolers. We also discuss simplifications and limitations of the current work.

A common practice nowadays is to add radiative cooling solutions on the roofs or the existing building walls in order to cool these surfaces. This retrofit is particularly simple in the older buildings where window to surface ratio is relatively small. However, in the modern buildings there is a growing trend of increasing the window surface area for esthetic or architectural purposes, which can bring their specifications well outside of the optimal range value which can be modeled numerically and that depend significantly on the geographical location of the building, as well as building orientation [48]. Thus, buildings with a window-to-wall ratio over 70% are not uncommon, while the optimal range is often $< 30\%$ [49]. Due to esthetic and life quality importance of large windows, the problem of making such windows energy efficient is more acute than ever. So, even when covering the whole building with radiative coolers, it is still important to address the inefficiency of windows due to the large surface area that they occupy compared to that of the building walls. More importantly, window panels are strongly thermally coupled to the inside of the house, and are, in fact, the weakest link when it comes to energy loss in a building. Thus, even a small improvement in the window thermal performance could significantly affect the building energy efficiency. In contrast, radiative cooling panels that are commonly installed on the outside of the building walls might have less of an effect on the building thermal efficiency due to their weak thermal coupling to the building interior. This is because building walls are efficient thermal isolators. Additionally, due to stronger thermal coupling, improvement in the window performance should also have a faster effect on the building interior temperatures due to a cyclic dynamic variation of the external heat fluxes and temperatures. Therefore, we believe that window/radiative cooler tandem solution should have superior static and dynamic effects on the building thermal efficiency compared to an externally mounted radiative cooler. This question, however, should be studied further.

One important engineering challenge of the proposed technology is the use of coolant liquid for thermal exchange between the cooler and window panels. Beyond an obvious challenge of hermetic sealing of the panels to prevent liquid leakage, a more significant challenge is that such panels are relatively thin and might not be good thermal isolators. This means that due to potentially significant convection of air at the panel external interfaces, the coolant liquid can be thermally coupled to the environment via thermal conduction through the panel material, resulting in significant drop in efficiency of the radiative panel/window heat exchange. Therefore, practical implementation of the physical principals described in this paper will require efficient thermal isolation of the coolant liquid from the convective thermal exchange at the panel outer surfaces. This can be readily achieved by using a variety of currently available high-performance windows, such as vacuum-insolated (evacuated) windows which are good thermal isolators, or most recently developed aerogel-insolated windows which are excellent thermal isolators [50]. Thus, surrounding the coolant liquid on both sides with thermally isolating panels, an efficient heat exchange can be realized.

We would also like to note that this work was mostly aimed at detailing a new principle for the development of thermally efficient windows featuring high transmission of the visible light. To simplify our presentation, we resorted to highlighting the physical reasoning behind such designs by using simplified 1D models for the radiative heat transfer. Naturally, in adapting such an approach the engineering aspect as well as a 3D aspect of the real world were not fully featured in our estimates, thus resulting in potential overestimation of the performance of our devices. For example, we predict that an ideal radiative cooler is capable of operating at $0.94\,T_a$, which is $\sim 18^\circ$C below ambient, while in practice the highest reported temperature drops using radiative cooling in open-air condition are $\sim 5^\circ\text{C} - 10^\circ\text{C}$. At the same time, in this work we wanted to keep the presentation as simple as possible; therefore, we believe that the use of simple 1D models together with the ideal materials is justified, while the obtained results should be rather considered as the theoretical bounds of the technology performance against which the real systems could be benchmarked.

Finally, we note that while coupling the radiative cooler and window panels into a single tandem does not result automatically in a "smart" window, there is certainly an element of "smart" functionality in the proposed design. In particular, an enhanced cooling function can be turned on during summer months by letting the coolant flow between the window and radiative cooler panels, while blocking such a flow during winter months when enhanced thermal isolation is of prime importance. We defer further investigation of other "smart" functionalities of the radiative cooler/window tandem to our future work.

6. CONCLUSION

We have considered several simple physical models of the radiative coolers and partially transparent radiative windows. We have then distinguished the design goals for these two structures and provided the optimal choice for the material parameters to realize these goals. Finally, we studied a thermally coupled window/radiative cooler system and showed how transmission of the visible light through the window can be enhanced without raising the window temperature above that of the ambient. Our findings can be summarized as follows.

Radiative cooling problem. Radiative coolers are normally non-transparent, and the main question is how to design a cooler so that the temperature on its dark side is as low as possible compared to that of the atmosphere. This is achieved when the window is almost perfectly reflective in the visible $R_w^{\text{VIS}} \to 1$ (alternatively $T_w^{\text{VIS}} \to 0$, $A_w^{\text{VIS}} \to 0$), and when window absorption loss in the visible is much smaller than that in the mid-IR $A_w^{\text{VIS}} \ll \varepsilon_w^{\text{MIR}}$. Then, in the absence of convection, and for any choice of the material optical parameters in the mid-IR $(T_w^{\text{MIR}},\ \varepsilon_w^{\text{MIR}})$ $\min(T_w) = \min(T_s) = \varepsilon_a^{0.25} \cdot T_a \approx 0.94\ T_a$. In the presence of convection, radiative cooling efficiency reduces potentially to zero when convection is strong.

Partially transparent radiative window problem. For the radiative windows, their surfaces are partially transparent, and the main question is rather about the maximal visible light transmission through the window at which the temperature on the window somber side does not exceed that of the atmosphere.

This is achieved when window transmission in the mid-IR is almost perfect $T_w^{\mathrm{MIR}} \to 1$ (alternatively $R_w^{\mathrm{MIR}} \to 0, \varepsilon_w^{\mathrm{MIR}} \to 0$), while window absorption in the visible is small $A_w^{\mathrm{VIS}} \to 0$ and at the same time much smaller than that in the mid-IR $A_w^{\mathrm{VIS}} \ll \varepsilon_w^{\mathrm{MIR}}$. Then, in the absence of convection, the maximal allowed transmission through the window in the visible is $T_w^{\mathrm{MIR}} = \gamma = (1-\varepsilon_a)/(2-\varepsilon_a) = 0.18$ while the wall, room, and window temperatures are all smaller than the atmospheric one. If only requiring that the room and window temperatures are smaller than the atmospheric one, then the maximal transmission through the window in the visible can be increased to $T_w^{\mathrm{VIS}} = 4\gamma/3 \approx 0.24$. In the presence of convection, the maximal allowed window transmission in the visible reduces somewhat (at most as a certain multiplicative factor) even in the presence of strong convection.

Effect of convection. Convection contribution becomes important for high enough values of the heat transfer coefficient $h \gg 8\sigma T_a^3 (2T_w^{\mathrm{MIR}} + \varepsilon_w^{\mathrm{MIR}})$, which for the standard ambient temperatures is equivalent to $h \gg 12[\mathrm{W/(m^2K)}] \cdot (2T_w^{\mathrm{MIR}} + \varepsilon_w^{\mathrm{MIR}})$. The value of the heat transfer coefficient depends strongly on the temperature differential between the window and the ambient temperatures, as well as the window size and orientation, and is generally in the 1–10 $[\mathrm{W/(m^2K)}]$ range for the non-forced convection.

Finally, by thermally coupling smart windows to radiative coolers using passive or active flows of a fluid coolant placed inside of the window and cooler structures, one can significantly increase transmission of the visible light through the window, while keeping the window temperature below that of the ambient. This enhancement is a function of the heat transfer rate per unit temperature ζ, and the largest enhancement is achieved in the limit of strong heat exchange between a window and a cooler $\zeta/4\sigma T_a^3 \gg (\varepsilon_w^{\mathrm{MIR}} \cdot \varepsilon_c^{\mathrm{MIR}})^{0.5}$, which for the standard ambient temperatures is equivalent to $\zeta \gg 6[\mathrm{W/(m^2K)}](\varepsilon_w^{\mathrm{MIR}} \cdot \varepsilon_c^{\mathrm{MIR}})^{0.5}$. Furthermore, a strong heat exchange regime between radiative coolers and smart windows can be realized with small coolant velocities (sub-1 mm/s for ~1 m large windows) or even using purely passive gravitationally driven coolant flows between a hot smart window and a cold radiative cooler mounted on top with minimal temperature differential (sub-1K) between the two.

Funding. l'Institut de l'énergie Trottier; Canada Research Chairs (Maksim Skorobogatiy).

Acknowledgment. Portions of this work were presented at the Iberoamerican Optics Meeting (RIAO) in 2019 as the OTh_5.8.

Disclosures. The authors declare no conflicts of interest.

REFERENCES

1. S. Sorrell, "Reducing energy demand: a review of issues, challenges and approaches," Renew. Sustain. Energy Rev. **47**, 74–82 (2015).
2. A. R. Kumar, K. Vijyakumar, and P. Sinivasan, "A review on passive cooling practices in residential buildings," Int. J. Math. Sci. Eng. Appl. **3**, 1–5 (2014).
3. M. M. Hossain and M. Gu, "Radiative cooling: principles, progress, and potentials," Adv. Sci. **3**, 1500360 (2016).
4. S. Catalanotti, V. Cuomo, G. Piro, D. Ruggi, V. Silvestrini, and G. Troise, "The radiative cooling of selective surfaces," Sol. Energy **17**, 83–89 (1975).
5. B. Zhao, M. Hu, X. Ao, N. Chen, and G. Pei, "Radiative cooling: A review of fundamentals, materials, applications, and prospects," Appl. Energy **236**, 489–513 (2019).
6. M. Santamouris, "Cooling the buildings–past, present and future," Energy Build. **128**, 617–638 (2016).
7. M. N. Bahadori, "Passive cooling systems in Iranian architecture," Sci. Am. **238**, 144–155 (1978).
8. C. Granqvist and A. Hjortsberg, "Radiative cooling to low temperatures: General considerations and application to selectively emitting SiO films," J. Appl. Phys. **52**, 4205–4220 (1981).
9. P. Berdahl and R. Fromberg, "The thermal radiance of clear skies," Sol. Energy **29**, 299–314 (1982).
10. T. Suichi, A. Ishikawa, Y. Hayashi, and K. Tsuruta, "Performance limit of daytime radiative cooling in warm humid environment," AIP Adv. **8**, 055124 (2018).
11. S. Long, H. Zhou, S. Bao, Y. Xin, X. Cao, and P. Jin, "Thermochromic multilayer films of WO3/VO2/WO3 sandwich structure with enhanced luminous transmittance and durability," RSC Adv. **6**, 106435 (2016).
12. N. DeForest, A. Shehabi, G. Garcia, J. Greenblatt, E. Masanet, E. S. Lee, S. Selkowitz, and D. J. Milliron, "Regional performance targets for transparent near-infrared switching electrochromic window glazings," Build. Environ. **61**, 160–168 (2013).
13. A. P. Raman, M. A. Anoma, L. Zhu, E. Rephaeli, and S. Fan, "Passive radiative cooling below ambient air temperature under direct sunlight," Nature **515**, 540–544 (2014).
14. P. F. Tavares, A. R. Gaspar, A. G. Martins, and F. Frontini, "Evaluation of electrochromic windows impact in the energy performance of buildings in Mediterranean climates," Energy Policy **67**, 68–81 (2014).
15. E. L. Runnerstrom, A. Llordés, S. D. Lounis, and D. J. Milliron, "Nanostructured electrochromic smart windows: traditional materials and NIR-selective plasmonic nanocrystals," Chem. Commun. **50**, 10555–10572 (2014).
16. P. Bamfield, *Chromic Phenomena: Technological Applications of Colour Chemistry* (RSC, 2010).
17. E. Rephaeli, A. Raman, and S. Fan, "Ultrabroadband photonic structures to achieve high-performance daytime radiative cooling," Nano Lett. **13**, 1457–1461 (2013).
18. T. P. Mann, "Metamaterial window glass for adaptable energy efficiency," Master's thesis (University of Texas at Austin, 2014).
19. S. Shin, S. Hong, and R. Chen, "Hollow photonic structures of transparent conducting oxide with selective and tunable absorptance," Appl. Therm. Eng. **145**, 416–422 (2018).
20. H. Ye, X. Meng, L. Long, and B. Xu, "The route to a perfect window," Renew. Energy **55**, 448–455 (2013).
21. Z. Chen, L. Zhu, A. Raman, and S. Fan, "Radiative cooling to deep sub-freezing temperatures through a 24-h day–night cycle," Nat. Commun. **7**, 13729 (2016).
22. P. Berdahl, "Radiative cooling with MgO and/or LiF layers," Appl. Opt. **23**, 370–372 (1984).
23. A. R. Gentle and G. B. Smith, "Radiative heat pumping from the earth using surface phonon resonant nanoparticles," Nano Lett. **10**, 373–379 (2010).
24. J. Yang, Z. Xu, H. Ye, X. Xu, X. Wu, and J. Wang, "Performance analyses of building energy on phase transition processes of vo2 windows with an improved model," Appl. Energy **159**, 502–508 (2015).
25. C. Granqvist, "Chromogenic materials for transmittance control of large-area windows," Crit. Rev. Solid State **16**, 291–308 (1990).
26. C. G. Granqvist, S. Green, G. A. Niklasson, N. R. Mlyuka, S. Von Kraemer, and P. Georén, "Advances in chromogenic materials and devices," Thin Solid Films **518**, 3046–3053 (2010).
27. C. G. Granqvist, G. A. Niklasson, and A. Azens, "Electrochromics: fundamentals and energy-related applications of oxide-based devices," Appl. Phys. A **89**, 29–35 (2007).
28. L. Long and H. Ye, "Dual-intelligent windows regulating both solar and long-wave radiations dynamically," Sol. Energy Mater. Sol. Cells **169**, 145–150 (2017).
29. H. Hillmer, B. Al-Qargholi, M. M. Khan, N. Worapattrakul, H. Wilke, C. Woidt, and A. Tatzel, "Optical mems-based micromirror arrays

for active light steering in smart windows," Jpn. J. Appl. Phys. **57**, 08PA07 (2018).
30. B. A. Korgel, "Materials science: composite for smarter windows," Nature **500**, 278–279 (2013).
31. A. Llordés, G. Garcia, J. Gazquez, and D. J. Milliron, "Tunable near-infrared and visible-light transmittance in nanocrystal-in-glass composites," Nature **500**, 323–326 (2013).
32. L. Long and H. Ye, "How to be smart and energy efficient: A general discussion on thermochromic windows," Sci. Rep. **4**, 6427 (2014).
33. H. Ye, X. Meng, and B. Xu, "Theoretical discussions of perfect window, ideal near infrared solar spectrum regulating window and current thermochromic window," Energy Build. **49**, 164–172 (2012).
34. M. E. Warwick and R. Binions, "Advances in thermochromic vanadium dioxide films," J. Mater. Chem. A **2**, 3275–3292 (2014).
35. Y. Zhan, X. Xiao, Y. Lu, Z. Cao, S. Qi, C. Huan, C. Ye, H. Cheng, J. Shi, X. Xu, and G. Xu, "The growth mechanism of vo2 multilayer thin films with high thermochromic performance prepared by RTA in air," Surf. Interfaces **9**, 173–181 (2017).
36. M. Liu, B. Su, Y. V. Kaneti, Z. Chen, Y. Tang, Y. Yuan, Y. Gao, L. Jiang, X. Jiang, and A. Yu, "Dual-phase transformation: Spontaneous self-template surface-patterning strategy for ultra-transparent VO2 solar modulating coatings," ACS Nano **11**, 407–415 (2016).
37. B. Zhu, H. Tao, and X. Zhao, "Effect of buffer layer on thermochromic performances of VO2 films fabricated by magnetron sputtering," Infrared Phys. Technol. **75**, 22–25 (2016).
38. F. Xu, X. Cao, H. Luo, and P. Jin, "Recent advances in VO2-based thermochromic composites for smart windows," J. Mater. Chem. C **6**, 1903–1919 (2018).
39. J. Zhang, H. He, Y. Xie, and B. Pan, "Theoretical study on the tungsten-induced reduction of transition temperature and the degradation of optical properties for VO2," J. Chem. Phys. **138**, 114705 (2013).
40. S. J. Lee, D. S. Choi, S. H. Kang, W. S. Yang, S. Nahm, S. H. Han, and T. Kim, "VO2/ WO3–based hybrid smart windows with thermochromic and electrochromic properties," ACS Sustain. Chem. Eng. **7**, 7111–7117 (2019).
41. J. Mandal, S. Du, M. Dontigny, K. Zaghib, N. Yu, and Y. Yang, "Li4Ti5O12: A visible-to-infrared broadband electrochromic material for optical and thermal management," Adv. Funct. Mater. **28**, 1802180 (2018).
42. G. K. Dalapati, A. K. Kushwaha, M. Sharma, V. Suresh, S. Shannigrahi, S. Zhuk, and S. Masudy-Panah, "Transparent heat regulating (THR) materials and coatings for energy saving window applications: Impact of materials design, micro-structural, and interface quality on the THR performance," Prog. Mater. Sci. **95**, 42–131 (2018).
43. A. Berk, P. Conforti, R. Kennett, T. Perkins, F. Hawes, and J. Van Den Bosch, "MODTRAN 6: a major up-grade of the MODTRAN radiative transfer code," in *6th Workshop on Hyperspectral Image and Signal Processing: Evolution in Remote Sensing (WHISPERS)* (IEEE, 2014), pp. 1–4.
44. J. R. Howell, M. P. Menguc, and R. Siegel, *Thermal Radiation Heat Transfer* (CRC Press, 2015).
45. H. Kusaka, H. Kondo, Y. Kikegawa, and F. Kimura, "A simple single-layer urban canopy model for atmospheric models: comparison with multi-layer and slab models," Bound. Layer Meteorol. **101**, 329–358 (2001).
46. E. Zhang, Y. Cao, C. Caloz, and M. Skorobogatiy, "Improving thermo-optic properties of smart windows via coupling to radiative coolers," engrXiv preprint (2019).
47. E. A. Goldstein, A. P. Raman, and S. Fan, "Sub-ambient non-evaporative fluid cooling with the sky," Nat. Energy **2**, 17143 (2017).
48. H. Alibaba, "Determination of optimum window to external wall ratio for offices in a hot and humid climate," MDPI Sustainability **8**, 187 (2016).
49. http://mundobim.com/construpm/edge-green-buildings-whats-window-to-wall-ratio/.
50. https://www.commercialwindows.org/adv_glass.php.